# THE EFFECTS OF JITTERS ON COHERENT X-RAY RADIATION USING A MODULATION COMPRESSION SCHEME*

J. Qiang†, LBNL, Berkeley, CA 94720, USA
J. Wu, SLAC, Menlo Park, CA 94025, USA

*Abstract*

Modulation compression scheme using a chirped beam, laser modulator and laser chirper, and a sequence of bunch compressors and radiators was recently proposed to generate coherent multi-color attosecond X-ray radiation [1]. In this paper, we will present studies of effects of the initial longitudinal beam energy chirp jitter, time synchronization jitter between the electron beam and the laser chirper, and the laser chirper amplitude jitter on the final coherent X-ray radiation. Connection between the modulation compression scheme and the echo scheme will also be briefly discussed.

## INTRODUCTION

Ultra-short coherent X-ray sources have important applications in biology, chemistry, condense matter physics, and material science. In recent years, there are growing interests in generating single attosecond x-ray radiation using Free Electron Lasers (FELs) [2, 3, 4, 5, 6, 7, 8, 9]. Meanwhile, multi-color attosecond X-ray radiation has important applications in time-resolved experiments such as multidimensional X-ray spectroscopy by either exciting or probing different types of atom in a system [10]. In our previous studies, modulation compression scheme was proposed to compress the initial laser modulation to generate short wavelength attosecond X-ray radiation [11, 12, 13, 1]. Especially, in reference [1], a scheme to generate multi-color attosecond X-ray radiation was proposed. This scheme consists of a chirped electron beam, a modulator, a bunch compressor, a laser chirper, and a sequence of bunch compressors and undulator radiators. An example to generate two color X-ray radiations was presented in the reference [1]. Using a 50 Ampere 200 nm laser seeded electron beam, two attosecond coherent X-ray radiation pulses with a wavelength of 2.2 nm and 3 nm and more than 200 MW peak power were generated under the nominal design parameters. In this paper, we study the effects of deviations from the nominal parameters due to various jitters in the above proposed scheme on the final X-ray radiation.

A schematic plot of the scheme to generate multi-color attosecond X-ray radiation is given in Fig. 1. It consists of an energy chirped electron beam, a seeding laser modulator, a bunch compressor A, a laser chirper, a bunch compressor B1, an undulator radiator one, a bunch compressor B2, another undulator radiator two, and a sequence of repeating bunch compressors and radiators to generate multi-color X-ray radiation. Here, a laser chirper is a laser modulator that is used to provide local energy chirp to an electron beam. Assume the initial longitudinal phase space distribution of the beam as $f(z,\delta) = F(z,(\delta - hz)/\sigma)$, where $z$ is the relative longitudinal coordiante with respect to the reference particle, $\delta = \Delta E/E$ is the relative energy deviation, $h$ is the initial beam energy chirp, and $\sigma$ is the initial uncorrelated energy spread. By properly choosing the momentum compaction factor of the bunch compressor B such that

$$R^b_{56} = -R^a_{56}/M \tag{1}$$

the longitudinal phase space distribution after the bunch compressor B1 can be written as:

$$f(z,\delta) = F(Mz,[\delta - M\tilde{h}z - MA\sin(kMz)]/M\hbar) \tag{2}$$

where

$$M = 1 + h_b R^a_{56} \tag{3}$$

represents the total modulation compression factor, $\hbar = h_b/C + h$, $C$ is the compression factor from the first bunch compressor A, $h_b$ is the energy chirp introduced by the laser chirper, $R^a_{56}$ is the momentum compaction factor of the first bunch compressor, $A$ is the modulation amplitude of the seeding laser in the unit of the relative energy, and $k$ is the wave number of the seeding laser. The above distribution function represents a compressed modulation in a chirped beam. In the above equations, we have also assumed a longitudinally frozen electron beam and a linear laser chirper instead of the real sinusoidal function from the laser modulator.

The linear chirp in Eq. 3 from a sinusoidal laser chirper modulation can be approximated as $h_b = A_b\, k_b$, where $A_b$ is the amplitude of the laser modulation, $k_b$ is the wavenumber of the laser. The sinusoidal form of the energy modulation provides periodical energy chirping/unchirping across the beam. If the amplitude envelop of the sinusoidal energy modulation is controlled externally, the periodical

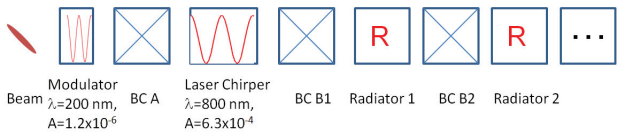


Figure 1: A schematic plot of the lattice layout of the modulation compression scheme.

* Work supported by the Office of Science of the U.S. Department of Energy under Contract No. DE-AC02-05CH11231.
† jqiang@lbl.gov



ISBN 978-3-95450-117-5

local chirping of the beam can be controlled. From Eq. 3, the local modulation compression factor can be controlled across the beam. This results in a periodically separated locally modulated beam with different modulation wavelengths. For a Gaussian laser beam, the energy modulation caused by the laser chirper is assumed as:

$$\delta = \delta + A_b \sin(k_b z) \exp(-\frac{1}{2}\frac{z^2}{\sigma_b^2}) \quad (4)$$

where $\sigma_b$ is the rms laser pulse length. The local linear chirp resulted from such a laser chirper at different wavelength separation will be

$$h_b(n\lambda) = A_b k_b \exp(-\frac{1}{2}\frac{(n\lambda)^2}{\sigma_b^2}) \quad (5)$$

where $n = 0, \pm 1, \pm 2, \cdots$. Using Eq. 3, the resultant modulation compression factor $M$ becomes

$$M(n\lambda) = 1 + A_b k_b \exp(-\frac{1}{2}\frac{(n\lambda)^2}{\sigma_b^2}) R_{56}^a \quad (6)$$

From above equation, we see that on either side of the Gaussian laser pulse (i.e. $n \geq 0$, or $n \leq 0$), the compressed modulation wavelength will decrease with the increase of the separation. To achieve the final modulation compression, the $R_{56}^b$ of the bunch compressor Bs after the laser chirper needs to match the condition Eq. 1. For the first local chirp $h_b(0)$, this can be done by using the bunch compressor B1. After the beam passes through the first radiator to generate first color radiation, the second bunch compressor B2 can be used to produce locally prebunched beam corresponding to the local chirp $h_b(\lambda)$. Such a locally prebunched beam passing through the second radiator will generate another color X-ray. Following the same procedure, multi-color X-ray radiation can be generated by using multiple bunch compressor and radiator pairs for different local chirp $h_b$ and modulation compression factor.

## EFFECTS OF JITTERS ON MULTI-COLOR ATTOSECOND X-RAY RADIATION

In this study, we use the same parameters as those used in the reference [1] example. A short uniform electron bunch (100 $\mu$m) with 17 pC charge, 2 GeV energy, $-54.45$ m$^{-1}$ energy-bunch length chirp, and an uncorrelated energy spread of $1 \times 10^{-6}$ is assumed at the beginning of the seeding laser modulator of 200 nm wavelength. The initial normalized modulation amplitude $A$ is $1.2 \times 10^{-6}$. Previous study under nominal idealized conditions showed that two attosecond X-ray radiation pulses with wavelengths of 2.2 nm and 3 nm and more than 200 MW peak power could be generated using a modulation compressed beam passing through two radiators. In practical application, there exist various jitters of beam and laser that could affect the performance of the final X-ray radiation. Those jitters include the time synchronization error between the electron beam and the chirper laser, the initial electron beam energy_ bunch length chirp error, and the chirper laser field amplitude error.

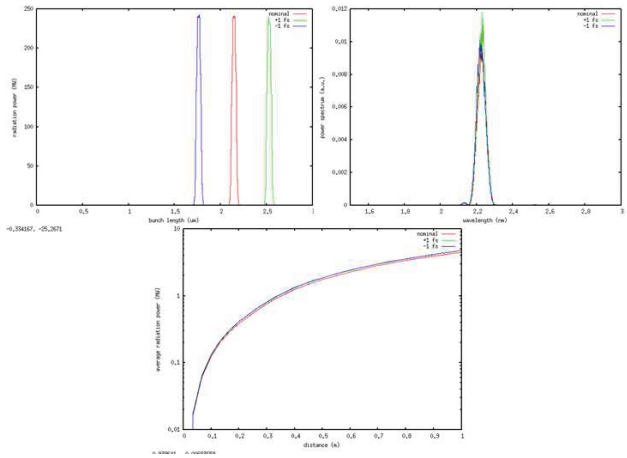

Figure 2: X-ray radiation power temporal profile (top left), power spectrum (top right) at the end of the radiator one, and average power evolution (bottom) without and with one femtosecond time synchronization error.

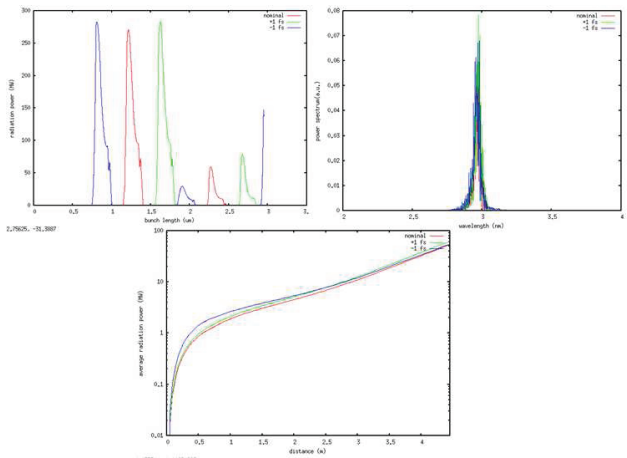

Figure 3: X-ray radiation power temporal profile (top left), power spectrum (top right) at the end of the radiator two, and average power evolution (bottom) without and with one femtosecond time synchronization error.

We first check the effects of the synchronization jitter between the laser and the electron beam. We assume that there is 1 fs delay or ahead between the laser and the electron beam inside the laser chirper compared with the nominal design. We follow the same procedure as described in the reference [1], where the longitudinal electron particle distribution out of the bunch compressor BC1 is sent into the radiator one assuming 0.2 mm-mrad transverse emittance. The X-ray radiation process inside the radiator is simulated using the time-dependent FEL code, GENESIS [14]. The particle longitudinal distribution at the end of the radiator one from the GNEESIS output is used to transport through the bunch compressor BC2 and then in-



ISBN 978-3-95450-117-5

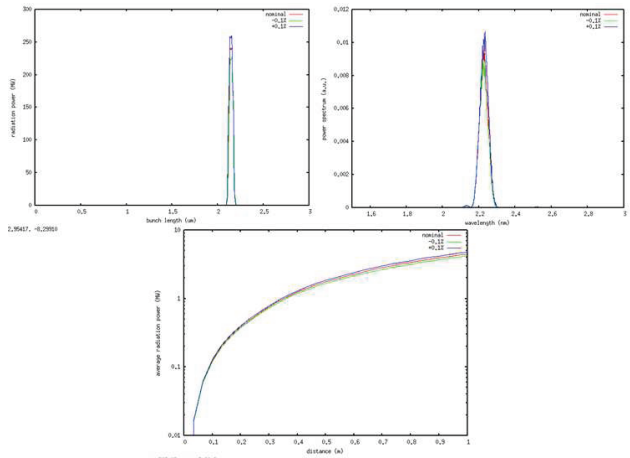

Figure 4: X-ray radiation power temporal profile (top left), power spectrum (top right) at the end of radiator one, and average power evolution (bottom) without and with 0.1% initial beam energy chirp jitter.

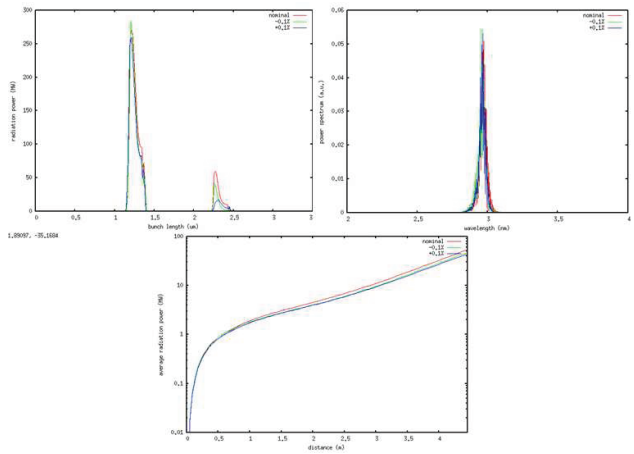

Figure 5: X-ray radiation power temporal profile (top left), power spectrum (top right) at the end of radiator two, and average power evolution (bottom) without and with 0.1% initial beam energy chirp jitter.

put into another GENESIS simulation through the radiator two. Figure 2 and Fig. 3 show the attosecond X-ray radiations at the end of the radiator one and two and the average radiation power through the two radiators. It is seen that except the shift of radiation temporal pulse location inside the beam, there is little change of radiation temporal profile, power spectrum, and average power evolution between the nominal radiation and the radiations with 1 fs synchronization time jitter. We also simulated a time deviation of 5 fs between the laser and the electron beam, the final radiation power variation is still very small. The slight shift of the radiation wavelength due to the change of resonance energy inside the radiator is also inside the radiation wavelength bandwidth. It is noted that the electron beam after the bunch compressor A will acquire a large global energy chirp due to the compression. The synchronization error between the electron beam and the laser results in the shift of the center energy of the modulation compressed beam after the laser chirper. For a short radiator, this shift of the center resonance energy stays inside the resonance bandwidth and hence produces less impact to the final X-ray radiation as shown in above figures.

Next, we consider the effects of the initial beam global energy chirp jitters on the X-ray radiation. This error is mainly due to the RF phase and amplitude jitters inside the linac that accelerates the beam. The initial energy chirp jitter causes the current jitter after the bunch compressor A. For a compression factor of 25 through the bunch compressor A, a 0.1% fluctuation of the initial energy chirp will result in a few percentage of fluctuation of beam current after the bunch compressor. This fluctuation will cause the fluctuation of final X-ray radiation power. Figure 4 and 5 show the X-ray radiation power temporal profiles and power spectrum at the end of the radiator one and two and the average power evolution through the radiators with the nominal initial energy chirp and with the 0.1% off the nominal value. With the 0.1% initial beam energy chirp deviation from the nominal value, the X-ray radiation power shows less than 10% deviation from the nominal radiation power. The radiation wavelength shows slight variation at the end of both radiators and is well within the nominal radiation wavelength bandwidth. We also ran simulations with 0.5% initial beam energy chirp jitter. This jitter causes less than 30% variation of the final X-ray radiation power.

Last, we check the effects of laser field jitter on the final X-ray radiation. The laser power used in the laser chirper can also have fluctuation. This makes the laser field in the laser chirper deviate from the nominal value used in the reference [1] example. The fluctuation of the laser amplitude causes the fluctuation of the final modulation compression factor, hence the radiation wavelength. However, with 0.1% level of fluctuation, the final wavelength fluctuation can be controlled within the nominal radiation bandwidth that is on the level of 1%. Figure 6 and 7 show the X-ray radiation power temporal profiles and spectrum at the end of the radiator one and two, and the average power evolution inside the radiators with the nominal field amplitude and with the 0.1% deviation from the nominal value. With the 0.1% laser field deviation from the design value, the final X-ray radiation power show small variation ($\sim$ %) from the nominal radiation power. Increasing the deviation to 0.5% produces less than 20% of the final radiation power fluctuation. The X-ray radiation wavelength still stays inside the wavelength bandwidth with above laser field amplitude jitters.

## THE MODULATION COMPRESSION AND THE ECHO SCHEME

In above study, we studied the effects of jitters on X-ray radiation in a modulation compression scheme. These results might be also valid for the echo scheme [15]. In

ISBN 978-3-95450-117-5

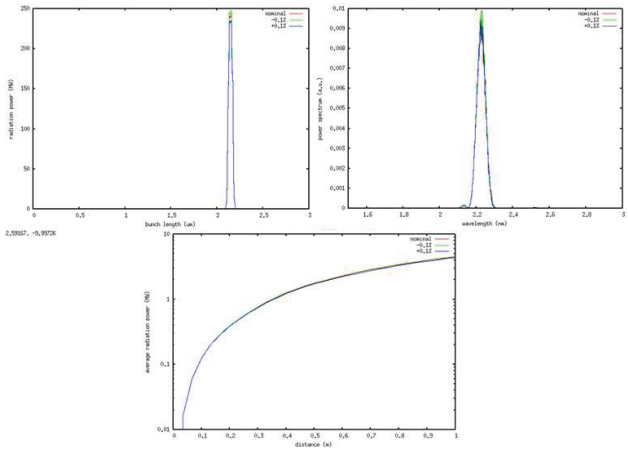

Figure 6: X-ray radiation power temporal profile (top left), power spectrum (top right) at the end of radiator one, and average power evolution (bottom) without and with 0.1% laser field amplitude jitter.

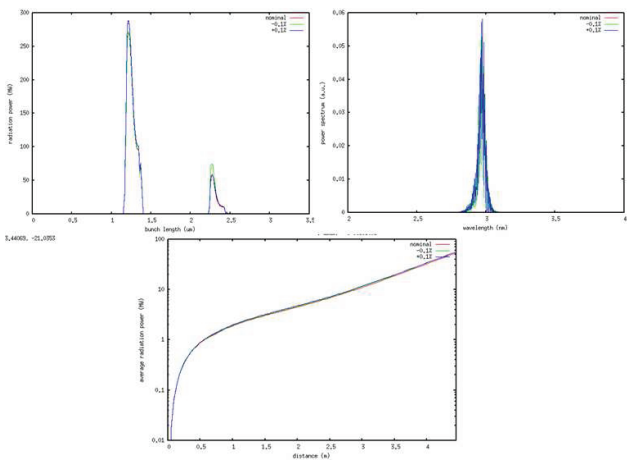

Figure 7: X-ray radiation power temporal profile (top left), power spectrum (top right) at the end of radiator two, and average power evolution (bottom) without and with 0.1% laser field amplitude jitter.

Fig. 1, using an initial beam chirp $h = 0$, choosing $h_b$ so that $M < 0$ (bunch compressor A and bunch compressor B1, $\cdots$ will have the same sign), then the modulation compression scheme becomes the echo scheme. The purpose of initial beam chirp has two folds: provides compression of the initial current from tens Ampere to thousands Ampere, and reduces the initial seeding modulation amplitude so that a significant number of the initial modulated electrons will fall into the compression of the laser chirper and the bunch compressor B1. A detailed study of the connection between the modulation compression scheme and the echo scheme for FEL short-wave seeding will be presented in our future publication.

## ACKNOWLEDGEMENTS

We would like to thank Drs. J. Corlett, J. Wurtele, A. Zholents for useful discussions. This research used computer resources at the National Energy Research Scientific Computing Center and at the National Center for Computational Sciences. The work of JW is supported by the U.S. Department of Energy under contract DE-AC02-76SF00515.

## REFERENCES

[1] J. Qiang, J. Wu, to appear in Appl. Phys. Lett. (2011).

[2] A. A. Zholents and W. M. Fawley, Phys. Rev. Lett. 92, 224801 (2004).

[3] A. A. Zholents and G. Penn, Phys. Rev. ST Accel. Beams 8, 050704 (2005)

[4] E. L. Saldin, E. A. Schneidmiller, and M. V. Yurkov, Phys. Rev. ST Accel. Beams 9, 050702 (2006)

[5] J. Wu, P. R. Bolton, J. B. Murphy, K. Wang, Optics Express 15, 12749, (2007).

[6] A. A. Zholents and M. S. Zolotorev, New Journal of Physcis 10, 025005 (2008).

[7] Y. Ding, Z. Huang, D. Ratner, P. Bucksbaum, and H. Merdji Phys. Rev. ST Accel. Beams 12, 060703 (2009).

[8] D. Xiang, Z. Huang, and G. Stupakov Phys. Rev. ST Accel. Beams 12, 060701 (2009).

[9] A. A. Zholents and G. Penn, Nucl. Instrum. Methods Phys. Res., Sec A 612, 254 (2010).

[10] S. Tanaka, and S. Mukamel, Phys. Rev. Lett., **89**, 043001 (2002).

[11] J. Qiang, NIM-A 621, p. 39, (2010).

[12] J. Qiang, J. Wu, to appear in J. Mod. Optics (2011).

[13] J. Qiang, J. Wu, Nucl. Instrum. Methods in Phys. Res., Sec A 640, p. 228 (2011).

[14] S. Reiche, Nucl. Instr. and Meth. A **429**, 243 (1999).

[15] G. Stupakov, Phys. Rev. Lett **102**, 074801 (2009).



ISBN 978-3-95450-117-5